Three-Dimensional MR-SPECT and MR-CT Registration Using a New Automated Method.

Panayiotis Kotsas and Michael G. Strintzis, *Senior Member IEEE*

Information Processing Laboratory

Department of Electrical and Computer Engineering

Aristotle University

54006 Thessaloniki

Greece

Abstract

A new technique for three-dimensional image registration has been developed and tested using MR, CT and SPECT image studies of the head. The method uses the fuzzy c-means classification algorithm for the definition of the registrable areas and then minimizes iteratively the mean squared value of the voxel per voxel weighted ratio of the two trilinearly interpolated cubic voxel volumes. A total of 80 three-dimensional registration experiments for SPECT to MR and CT to MR registration were performed and showed that the method is independent of signal intensity. The average registration accuracy is better than 1 degree for rotations and 1 mm for translations. The method has also been implemented hierarchically and performed well at low resolutions. The fastest hierarchical implementation improved the speed of the registration procedure by 57.5 percent on the average.

Keywords: image, registration, hierarchical, automated.

1. Introduction

Medical imaging modalities (Computed Tomography, Magnetic Resonance, Positron Emission Tomography, Single Photon Emission Computed Tomography) provide information that illustrates human brain anatomy and function. This information is often complementary and its correlative use can improve diagnostic accuracy. For example, the merging of fine anatomic detail from MR images of the brain with functional PET images allows the measurement of regional cerebral function[21]. Likewise, MR and CT images describe complementary morphologic features. Bone calcifications are seen best on CT images, while soft tissue structures are differentiated better by MR[18].

Medical image registration is the procedure of geometrically aligning two image volumes so that voxels representing the same anatomical structure may be superimposed one on another[15]. Registration techniques make it possible to superimpose features from one image study on those of another image study from a different modality. These techniques can also be applied to studies of the same modality taken at different times so that point-by-point arithmetic operations such as image averaging, subtraction and correlation can be performed [5].

In recent years there has been a rapid growth of neurological applications of medical image registration with applications that address both diagnosis and therapy. Registration is progressively playing a larger role in image interpretation in many different procedures.

Feature-based methods use the anatomic information inherent in the two image sets. These techniques follow a general methodology with four steps [13]:

a) extraction of features in each image

b) pairing of these features

c) choice of a geometric transformation and estimation of its parameters

d) application of this transformation.

Feature-based techniques do not require any special procedures or devices at imaging time and may be applied retrospectively [6,22]. The extraction of the anatomic features can be performed either manually with the assistance of an expert user or automatically. The disadvantages of interactive methods are that they require a large amount of time from the user and that the registration accuracy is affected by the user's performance.

Automated methods may be categorized according to their ability to perform cross-modality registration. Correlation methods [9,10] are not able to register image studies from different modalities because the signal intensity distributions differ. Principal axes [2,3] and surface fitting [2,8] methods use characteristics related to the shape of the two image volumes which are not affected by the difference in signal intensity distributions. Therefore these methods are able to perform cross-modality registration. Registration methods may also be categorized according to the way the geometric transformation parameters are estimated. The principal axes method gives a closed form

solution to the registration problem, whereas correlation and surface fitting methods solve the problem iteratively.

The purpose of this paper is to present a new automated, iterative method for the solution of the problem of three-dimensional cross-modality registration of medical images of the head. The rest of this paper is organized as follows: In Section 2 the registration methodology is presented. Section 3 presents the experimental protocols and gives the main results obtained for SPECT to MR and CT to MR registration. Conclusions are finally drawn in Section 4.

2. Methods

The implementation of the method for three-dimensional image registration uses the following processing steps:

I) Each of the scans of the two three-dimensional medical image studies is classified with the use of the fuzzy c-means classification algorithm as presented by Bezdek et al. [23]. Three clusters are used and a threshold for each scan is computed by taking the mean value of the centers of the two lowest clusters. This threshold is the value that separates the signal from the background area for each scan. The lowest of all thresholds computed for each study is adopted as the global threshold for this study. No thresholding operation is performed at this point.

II) The two studies are interpolated using a trilinear interpolation routine to create the cubic voxel volumes. This step is necessary because of the different resolution in the xy plane and the z axis used in the acquisition of three-dimensional medical image data.

III) All the voxel intensity values of the two volumes are compared to the global thresholds. If the signal intensity of a voxel is lower than the corresponding global threshold the voxel is assigned to the background.

IV) Finally, an iteration loop based on Chebyshev's approximation theory [25] is used to minimize the registration function, which is defined as the mean squared value of the average weighted ratio $\tilde{R}$ of the two volumes:

$$E\left(\tilde{R}^2\right) \quad \text{with} \quad \tilde{R} = \frac{1}{2} * \left(weighted(\frac{A}{B}) + weighted(\frac{B}{A}) \right) \quad [1]$$

where A and B are the two volumes. The ratios of the two volumes are computed on a voxel per voxel basis and weighting is performed by setting the voxel ratios with background voxels in the denominator to a standard high value. More specifically, the registration function is computed as follows:

Consider two three-dimensional digital images $A[i,j,k]$ and $B[i,j,k]$ with i:1...K, j:1...L, k:1...M. Using these images two ratios are defined, $R_1[i,j,k] = \frac{A[i,j,k]}{B[i,j,k]}$ and $R_2[i,j,k] = \frac{B[i,j,k]}{A[i,j,k]}$. Define now S to be an KxLxM image resulting from A or B by keeping nonzero values only for the signal voxels and as N an KxLxM image resulting from A or B by keeping nonzero values only for background voxels whose intensities are due to noise. The following relations hold $\forall$ i:1...K, j:1...L, k:1...M:

$$S[i,j,k] \neq 0 \Leftrightarrow N[i,j,k] = 0 \quad [2]$$

$$A[i,j,k] = S_A[i,j,k] + N_A[i,j,k] \quad [3]$$

$$B[i,j,k] = S_B[i,j,k] + N_B[i,j,k] \quad [4]$$

$$R_1[i,j,k] = \frac{S_A[i,j,k] + N_A[i,j,k]}{S_B[i,j,k] + N_B[i,j,k]} \quad [5]$$

$$R_2[i,j,k] = \frac{S_B[i,j,k] + N_B[i,j,k]}{S_A[i,j,k] + N_A[i,j,k]} \quad [6]$$

The weighted ratios $\tilde{R}_1$ and $\tilde{R}_2$ can now be defined as:

$$\tilde{R}_1[i,j,k] = \begin{cases} R_1[i,j,k] & \text{when } S_B[i,j,k] \neq 0 \\ C & \text{when } S_B[i,j,k] = 0 \end{cases} \quad [7]$$

$$\tilde{R}_2[i,j,k] = \begin{cases} R_2[i,j,k] & \text{when } S_A[i,j,k] \neq 0 \\ C & \text{when } S_A[i,j,k] = 0 \end{cases} \quad [8]$$

$$\forall\ i{:}1...\mathrm{K},\ j{:}1...\mathrm{L},\ k{:}1...\mathrm{M}$$

where C is a standard high value.

The function to be minimized iteratively is the mean squared value of the mean weighted ratio, that is :

$$E(\tilde{R}^2) \text{ with } \tilde{R}[i,j,k] = \frac{\tilde{R}_1[i,j,k] + \tilde{R}_2[i,j,k]}{2} \quad \forall\ i{:}1...\mathrm{K},\ j{:}1...\mathrm{L},\ k{:}1...\mathrm{M}$$

Figure 1 illustrates the meaning of the above relationships. The first line shows one MR scan and its rotation by 30 degrees. The second line left shows

the two above scans superimposed on each other and the second line right provides a mapping of the different types of areas that can be found in the mean weighted ratio image $\tilde{R}$. In the white area, the weighted ratios $\tilde{R}_1$ and $\tilde{R}_2$ are computed using signal voxels only, whereas in the gray area, one of the ratios is computed using background voxels in the denominator and this ratio is set to a standard high value. It is obvious that the gray area vanishes in the correct registration position. For this position, the registration function assumes its minimum value.

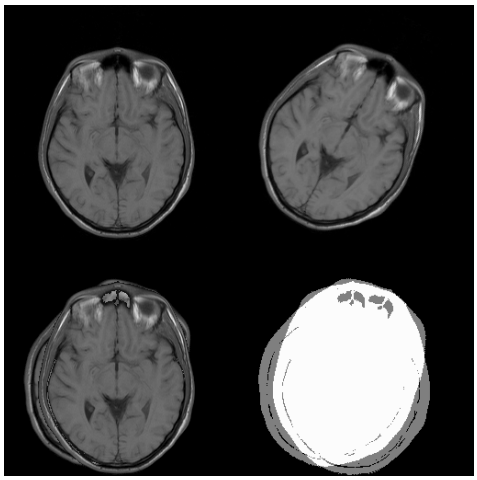

Figure 1: Illustration of the different image areas used by the algorithm for the computation of the registration function. First row: one scan and its rotation by 30 degrees. Second row: The two scans when superimposed give two different types of data. In the white area the registration function is computed with the use of signal voxels only, whereas in the gray area both signal and background voxels are used. The ratio of the two images is weighted by setting the ratio values in the gray area to a standard high value.

The registration function is minimized iteratively using the Chebyshev polynomial approximation theory [25]. The following steps define the main iteration loop:

1. One of the six possible geometric transformation parameters (three rotations around the three axes and three translations along the three axes) is adjusted with each iteration. In the experiments performed in this paper, the rotations preceded the translations.

2. One of the two volumes is defined as the *reference* volume. The other volume which is to be aligned to the reference volume will be referred to as the *reslice* volume because this volume has to be resliced after registration.

3. For each iteration the registration function is computed for n=5 Chebyshev points for the [-18,+18] transformation units interval. The transformation units are degrees for rotations and voxels for translations. The Chebyshev points used are [25]:

$$x_k = 18\cos\left(\frac{\pi(k-\frac{1}{2})}{n}\right) \qquad \text{k=1,...,n} \qquad [9]$$

For all other points in the range of the 36 transformation units, the registration function is approximated using the Chebyshev approximation formula:

$$f(x) \approx \left[\sum_{k=0}^{n-1} c_k T_k(x)\right] - \frac{1}{2}c_0 \qquad [10]$$

$T_k(x)$ is the Chebyshev polynomial of degree k and is given by the explicit formula:

$$T_k(x) = \cos(k \arccos(x)) \qquad [11]$$

The coefficients c_k are the Chebyshev coefficients and are defined by

$$c_k = \frac{2}{n}\sum_{l=1}^{n} f(x_l)T_k(x_l) \quad k=0,...,n-1 \qquad [12]$$

where x_l are the Chebyshev points.

The minimum of the approximated registration function fmin is considered as the adjustment value for the geometric transformation parameter.

4. A transformation parameter is determined to have converged when it completes a predetermined number of CONV iterations that give adjustment values smaller than one transformation unit. For the single-resolution experiments CONV was set to 2 but for the hierarchical implementation the value of CONV=1 was used in some cases for the higher resolution levels. The total adjustment value of the transformation parameter is the sum of all the adjustment values from all iterations used to adjust this parameter.

A block diagram of the registration method is shown in figure 2. Figure 3 illustrates the application of the fuzzy c-means classification method to an MR scan.

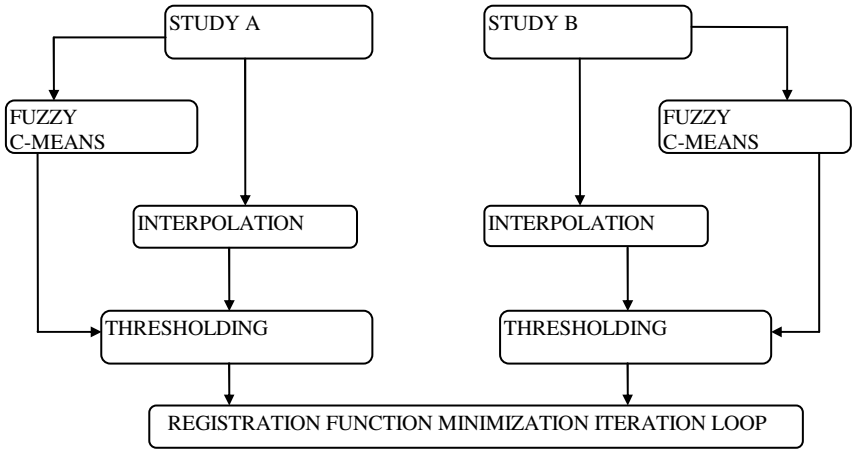

Figure 2: Block-diagram of the registration method.

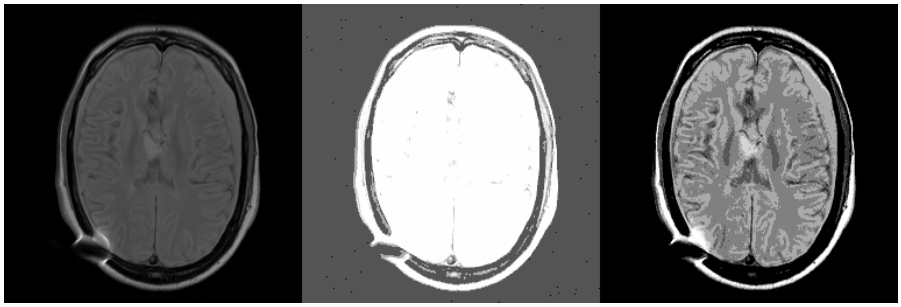

Figure 3: Application of the fuzzy c-means to an MR scan. Left: the original scan. Center: the c-means classified and defuzzified scan with c=3. Right: the c-means classified and defuzzified scan with c=7.

The method was also implemented hierarchically in the following way:

1. The images were subsampled by 4 along each of the 3 axes giving a cubic voxel size 4*S where S is the voxel size of the original images.

2. The registration algorithm was applied at this resolution and the adjustments computed were used as initial estimates for the registration of the images at the next resolution level (cubic voxel size 2*S).

3. The registration parameters computed at the half resolution level were used then as initial estimates for the final registration at the full resolution level (cubic voxel size S).

To better illustrate the registration procedure, a two-dimensional registration T2- to T1-weighted MR image registration experiment will be described in terms of the registration function curves, as they are extrapolated for the xy plane rotation parameter and for each iteration. Figure 4 shows the two scans before and after registration. The top left image is the T1 reference scan, the top right image is the T2 reslice scan before registration and the bottom left image is the reslice scan after registration. The errors computed for this experiment were 0.05 deg for xy rotation and 0.2 voxels for x translation and 1.8 voxels for y translation. Figures 5 to 7 show the variance curves with each iteration for rotational adjustment. The minimum values marked on the curves are the adjustment values that the algorithm uses to register the two images. The total adjustment is 37.68 deg, which corresponds to an error of 0.05 deg.

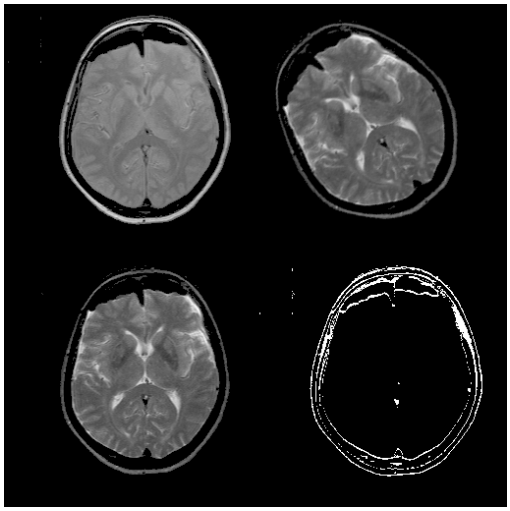

Figure 4: “20 displacement” T1-T2 registration example. Reference and reslice scans before and after registration. Top left: Reference T1 MR scan. Top right: Reslice T2 MR scan before registration. The two scans are rotated by 37.63 deg and translated by 23 voxels along the x-axis and 7 voxels along the y-axis. Bottom left: Reslice scan after registration. The registration error is 0.05 deg for xy rotation, 0.2 voxels for the x translation, and 1.85 voxels for the y translation. Bottom right: the white areas show the areas where the two scans do not overlap after registration.

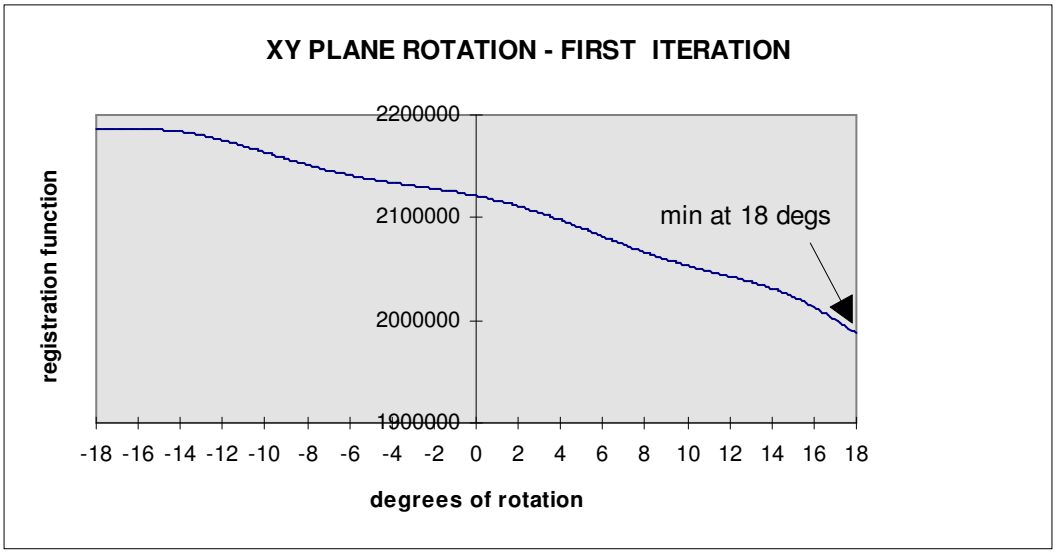

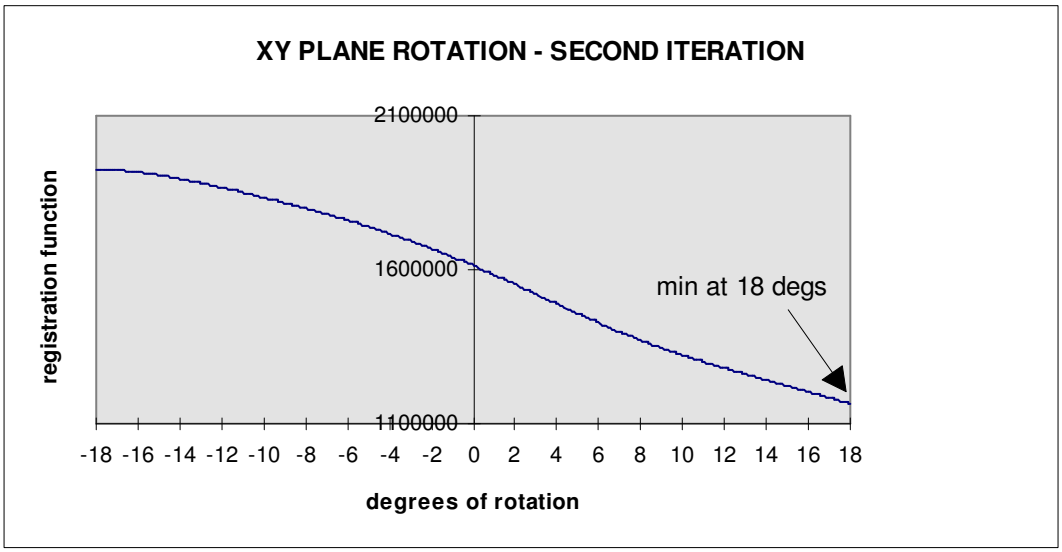

Figure 5: Two-dimensional T1-T2 registration example. Registration function minimization curves. Iterations 1 and 2.

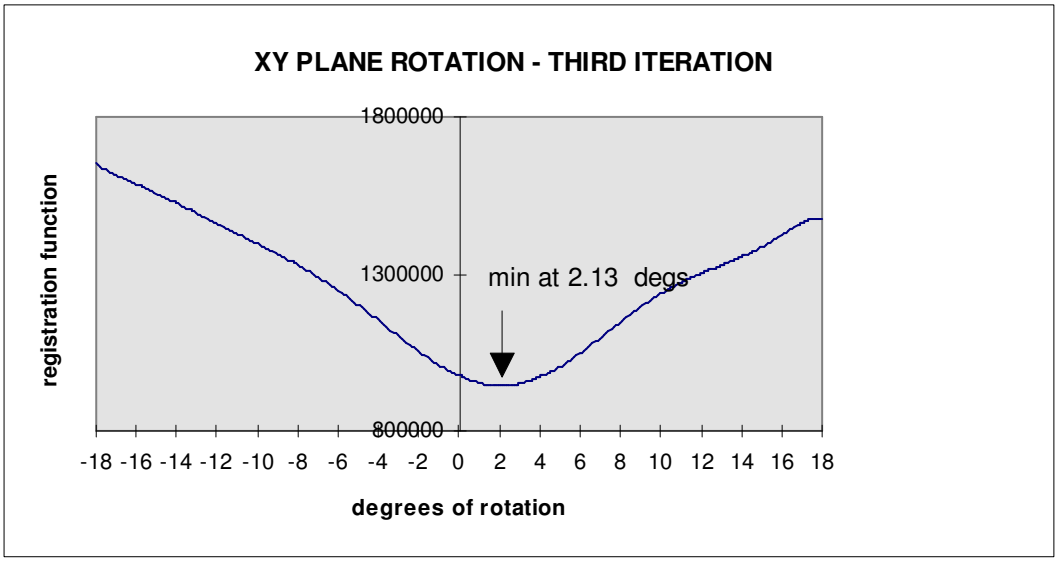

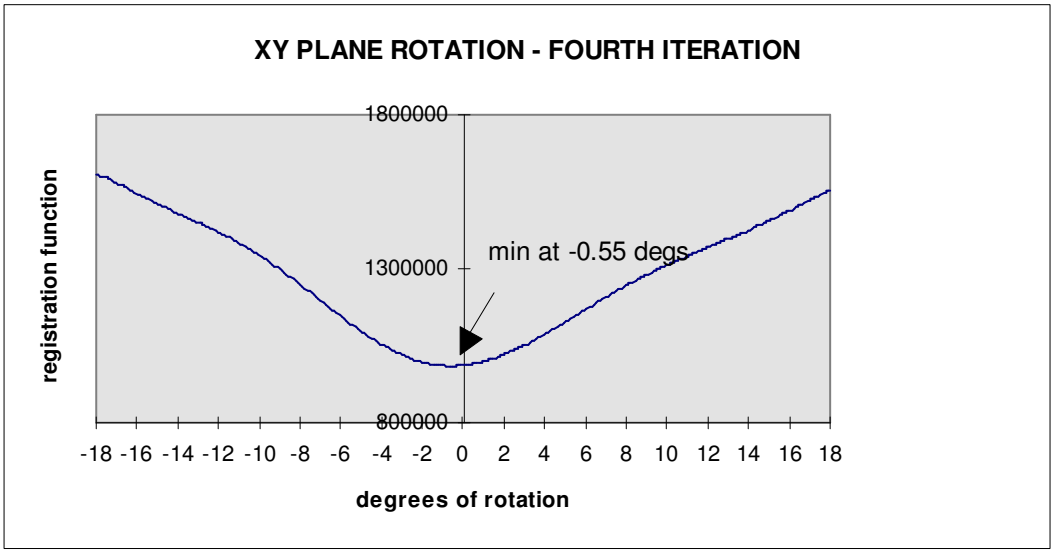

Figure 6:Two-dimensional T1-T2 registration example. Registration function minimization curves. Iterations 3 and 4.

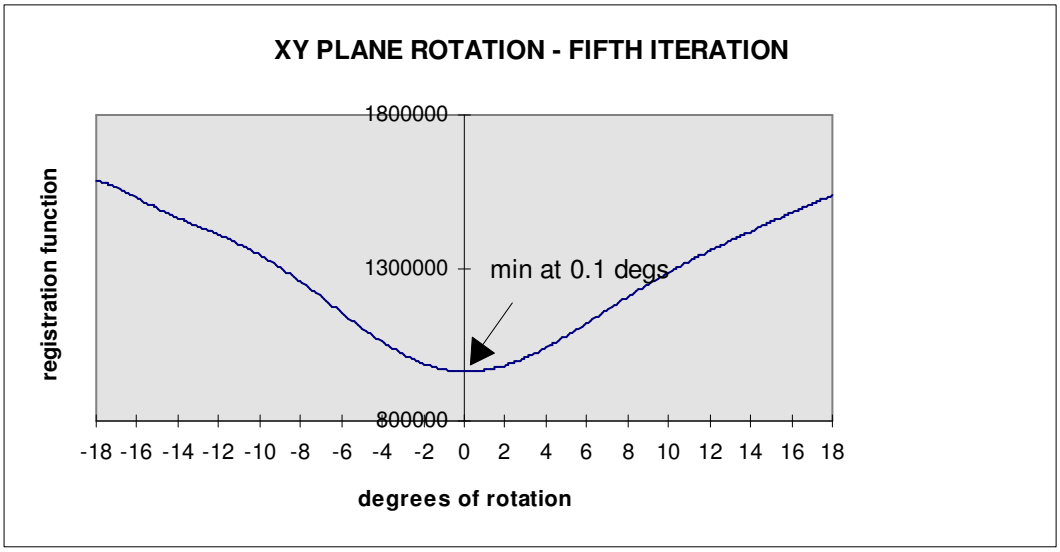

Figure 7: Two-dimensional T1-T2 registration example. Registration function minimization curve. Final iteration 5.
Total adjustment: 18+18+2.13-0.55+0.1 = 37.68 deg
Registration error: 37.68-37.63 = 0.05 deg

The application of the registration algorithm to the solution of the problem of three-dimensional registration of multi-modal (MR-CT and MR-SPECT) medical images of the head will be presented in the following Sections.

3. Experimental Protocols and Results

The method described in Section 1 was applied for SPECT to MR and CT to MR 3D registration. A total of 60 3D single-resolution and 20 3D hierarchical experiments were performed in order to estimate the accuracy of the method for cross-modality registration and test the performance of the hierarchical implementation of the method.

3.1 3D SPECT-MR registration

The SPECT and T2-weighted MR data used were obtained through "The Whole Brain Atlas" web page of the Harvard Medical School (http://count51.med.harvard.edu/AANLIB/home.html). The SPECT and MR studies came from a patient with metastatic bronchogenic carcinoma and are provided registered at http://count51.med.harvard.edu/AANLIB/cases/ /case28/mr1-tc1/010.html . Each study has 24 scans.

Using this data a total of 60 three-dimensional experiments for alignment of a SPECT to an MR study were performed. These experiments were conducted according to the following rules:

a) The MR study was used as the reference study. The SPECT study was considered the reslice study. The latter was rotated and translated using a standard set of 10 three-dimensional geometric transformations and then registered to the reference study, giving 10 registration experiments. For this reason these experiments will be referred to as "10 displacements" experiments. The rotational parameters of the geometric transformation set were randomly chosen within -30 degrees to +30 degrees for xy rotation, -10 degrees to +10 degrees for yz and zx rotations, -10 to +10 mm for x and y translations and -5 to +5 mm for z translation.

b) The *Absolute Error (AE)* per transformation parameter was defined as the absolute difference of the adjustment value from the transformation parameter value applied. The average of the AEs for the xy, yz, zx rotations was defined as the *Absolute Rotational Error (ARE)* per transformation and was computed in degrees. The *Absolute Translational Error (ATE)* per

transformation was computed in millimeters by averaging the x, y and z translation AEs in voxels and then by multiplying the average value by the voxel size (1.8 mm). The *Average Absolute Rotational Error (AARE)* per patient was defined as the average of the AREs from all transformations. Similarly, the *Average Absolute Translation Error (AATE)* per patient was defined as the average of the ATEs from all transformations.

The “10 displacements” registration experimental protocol is depicted in figure 8.

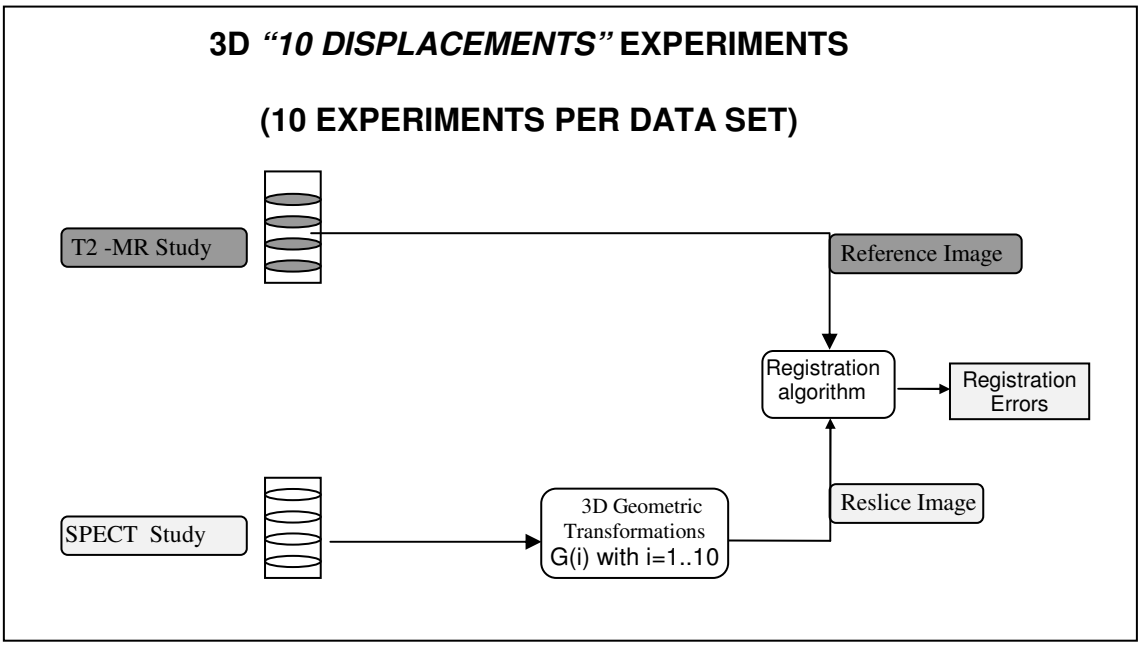

Figure 8: Experimental protocol used for the estimation of the 2D registration accuracy of the method for T1-T2 MR image registration.

The "10 displacements" experiments were first performed at 3 different resolutions (quarter, half, full) giving 30 single-resolution 3D SPECT-MR registration experiments. The Average Absolute Rotational and Translational Errors computed at each resolution are shown in Table 1. As expected, the best accuracy is obtained at full resolution with an AARE of 0.65 deg and AATE of 0.60mm. Only for quarter resolution the errors exceeded 1 deg and 1mm. Table 2 gives the Relative Average Processing Time for each resolution. It is computed by defining as To the time taken by the processor for each iteration

of the registration algorithm at full resolution and by considering the iteration times at half and quarter resolutions to be To/8 and To/64 respectively. Each entry of Table 7 is the average of the times computed for the 10 experiments. It can be seen that the ratio of the relative times computed for two consecutive resolution levels is close to 8. This result shows that the dynamic behavior of the algorithm, as measured by the number of iterations required for convergence, does not change with the resolution.

Table 1: Average Absolute Rotational and Translational Errors for the "10 displacements" single-resolution SPECT-MR 3D registration experiments for 3 different resolutions: quarter, half, full.

Resolution	**AARE (degrees)**	**AATE (mm)**
Quarter	1.68	1.51
Half	0.91	0.62
Full	0.65	0.60

Table 2: Relative Average Processing Time for the "10 displacements" single-resolution SPECT-MR 3D registration experiments for 3 different resolutions: quarter, half, full.

Resolution	**APT/To**
Quarter	0.26
Half	2.17
Full	19.3

The "10 displacements" experiments were repeated using the hierarchical form of the registration algorithm. The CONV parameter, which defines the number of less-than-1-unit iterations required for convergence of the transformation parameters, was modified in order to achieve a compromise between processing time and accuracy. Three different forms of hierarchy were used: the hier(2,2,2) form, where the value of CONV=2 was used at each resolution, the hier(2,2,1) form, where the value of CONV=1 was used for the full resolution level, and the hier(2,1,1) where the value of CONV=1 was used for resolutions half and full.

Tables 3a-c give the AARE and AATE and the Relative Average Processing Time for each resolution for the 3 hierarchical forms. Each entry of tables 3a-c is the average of 10 registration experiments.

Table 3a: AARE, AATE and Relative Average Processing Time for the "10 displacements" hierarchical SPECT-MR 3D registration experiments with the hier(2,1,1) scheme.

Resolution	AARE (degrees)	AATE (mm)	APT/To
Quarter	1.68	1.51	0.26
Half	1.22	0.73	0.9+0.26=1.16
Full	**0.94**	**0.46**	7.3+1.16=**8.46**

Table 3b: AARE, AATE and Relative Average Processing Time for the "10 displacement" hierarchical SPECT-MR 3D registration experiments with the hier(2,2,1) scheme.

Resolution	AARE (degrees)	AATE (mm)	APT/To
Quarter	1.68	1.51	0.26
Half	0.96	0.56	1.63+0.26=1.89
Full	**1.04**	**0.46**	6.3+1.89=**8.19**

Table 3c: AARE, AATE and Relative Average Processing Time for the "10 displacement" hierarchical SPECT-MR 3D registration experiments with the hier(2,2,2) scheme.

Resolution	AARE (degrees)	AATE (mm)	APT/To
Quarter	1.68	1.51	0.26
Half	0.96	0.56	1.63+0.26=1.89
Full	**0.65**	**0.61**	12.5+1.89=**14.39**

Tables 3a-c show that the hierarchical implementation reduced the processing time. The scheme (2,2,1) reduced the processing time by a factor of (1-8.19/19.3)=57.5% compared to the single-resolution method. The full hierarchical scheme hier(2,2,2) had the same accuracy as the single-resolution method while reducing the processing time by a factor of (1-14.39/19.3)=25.4%.

3.2 3D CT-MR registration

The CT and T2- MR data used, were obtained through "The Whole Brain Atlas" web page of the Harvard Medical School. The CT and MR studies came from a patient with acute stroke and are provided registered at http://count51.med.harvard.edu/AANLIB/cases/case2/ mr2/018.html . The "10 displacemenst" experimental protocol with the same transformations was

used for the CT-MR experiments. The T2-MR study was considered as the reference study and the CT study was considered as the reslice study. The brain area of the CT images was extracted using the Live Wire Tool of the 3DVIEWNIX software system and it was used as a mask in order to define the brain area in the T2-MR images. The CT study brain was then rotated and translated using the standard "10 displacements" transformation set and then registered to the reference MR study brain.

The hierarchical registration algorithm forms hier(2,2,1) and hier(2,2,2) that gave respectively the best registration speed and accuracy during the SPECT-MR experiments were tried. Tables 4a-b give the AARE and AATE and the Average Processing Time for each resolution for the 2 hierarchical forms. Each entry of tables 4a-b is the average of the 10 registration experiments.

Table 4a: AARE, AATE and Relative Average Processing Time for the "10 displacement" hierarchical CT-MR 3D registration experiments with the hier(2,2,1) scheme.

Resolution	AARE (degrees)	AATE (mm)	APT/To
Quarter	1.5	1.6	0.27
Half	0.82	0.83	1.5+0.27=1.77
Full	**0.68**	**0.51**	6+1.77**=7.77**

Table 4b: AARE, AATE and Relative Average Processing Time for the "10 displacement" hierarchical CT-MR 3D registration experiments with the hier(2,2,2) scheme.

Resolution	AARE (degrees)	AATE (mm)	APT/To
Quarter	1.5	1.6	0.27
Half	0.82	0.83	1.5+0.27=1.77
Full	**0.56**	**0.41**	12+1.77=**13.77**

Tables 4a-b show that the hier(2,2,2) form gives the best accuracy for both rotations (0.56 deg) and translations (0.41 mm). Its processing time however, was almost double the time needed by the hier(2,2,1) form.

4. Conclusions

We have presented the application of a new automated feature-based method for the solution of the problem of cross-modality registration of medical images. The method uses a Chebyshev polynomial approximation-based iteration loop to minimize a novel registration function which is defined as the mean-squared value of the weighted voxel-per-voxel mean ratio of the two images. Weighting is performed by setting the ratios between signal and background voxels to a standard high value. We used T2-weighted MR,

SPECT and CT image studies of the head and performed 80 three-dimensional registration experiments in order to evaluate the accuracy of the method for cross-modality registration and also to test the performance of the hierarchical form of the algorithm. We found that the average error for SPECT to MR registration is 0.65 deg for rotations and 0.6mm for translations. For CT to MR registration the average errors are respectively 0.56deg and 0.41mm. The dynamic behavior of the algorithm, as measured by the number of iterations taken for convergence, is not affected by the change in resolution. The hierarchical implementation improves the speed of the registration procedure by an average gain which is dependent on the hierarchical form used. The hier(2,2,2) form, which requires for convergence two iterations with adjustment values less than 1 transformation unit at all three resolution levels (quarter, half, full), retains the accuracy of the single-resolution method while improving the registration speed by 25.4 percent. The hier(2,2,1) form, which requires for convergence two less-than-1-unit iterations for quarter and half resolution and 1 less-than-1-unit iteration for full resolution, increased the registration speed by an average 57.5 percent.

In addition to providing excellent results, the proposed method is advantageous compared to cross-correlation techniques because it is independent of signal intensity distributions. It is also advantageous compared to least-squares based surface matching techniques because of its good behavior at lower resolutions and its tendency to avoid being trapped to local minima.

5. References

[1] P. Kotsas, "A New Automated Method for Three-Dimensional Registration of MR Images of the Head," *Master's Thesis*, Department of Biomedical Engineering, The Ohio-State University.

[2] H. Rusinek, W. H. Tsui, A. V. Levy, M. E. Noz and M. J. de Leon, "Principal axes and surface fitting methods for three-dimensional image registration," *J Nucl Med* 1993;34(11):2019-2024.

[3] N. M. Alpert, J. F. Bradshaw, D. Kennedy and J. A. Correia. "The principal axes transformation - A method for image registration," *J Nucl Med* 1990;31(10):1717-1722.

[4] P. J. Slomka, G. A. Hurwitz, J. Stephenson and T. Cradduck, "Automated alignment and sizing of myocardial stress and rest scans to three-dimensional normal templates using an image registration algorithm," *J Nucl Med* 1995;36(6):1115-1122.

[5] A. W. Toga, P. K. Banerjee. "Registration revisited," *J Neurosci Methods* 1993;48(1-2):1-13.

[6] T. G. Turkington, R. J. Jaszczak, C. A. Pelizzari, C. C. Harris, J. R. MacFall, J. M. Hoffman and R. E. Coleman , "Accuracy of registration of PET, SPECT and MR images of a brain phantom," *J of Nucl Med* 1993;34(9):1587-1594.

[7] T. G. Turkington, J. M. Hoffman, R. J. Jaszczak, J. R. MacFall, C. C. Harris, C. D. Kilts, C. A. Pelizzari and R. E. Coleman, "Accuracy of surface fit registration for PET and MR brain images using full and incomplete brain surfaces," *J Comput Assist Tomogr* 1995;19(1):117-124.

[8] C. A. Pelizzari, G. T. Chen, D. R. Spelbring, R. R. Weichselbaum and C. T. Chen. "Accurate three dimensional registration of CT, PET and/or MR images of the brain," *J Comput Assist Tomogr* 1989;13(1):20-26.

[9] L. Junck, J. G. Moen, G. D. Hutchins, M. B. Brown and D. E. Kuhl, "Correlation methods for the centering, rotation, and alignment of functional brain images," *J Nucl Med* 1990;31(7):1220-1226.

[10] Woods RP, Cherry SR and Mazziotta JC, "Rapid automated algorithm for aligning and reslicing PET images," *J Comput Assist Tomogr* 1992;16(4):620-633.

[11] Woods RP, Mazziotta JC and Cherry SR, "MRI-PET registration with automated algorithm," *J Comput Assist Tomogr* 1993;17(4):536-546.

[12] P. Gerlot-Chiron and Y. Bizais, "Definition and evaluation of a surface overlap criterion for medical image registration," *Prog Clin Biol Res* 1991;363: 429-442.

[13] P. Gerlot-Chiron and Y. Bizais, "Registration of multimodality medical images using a region overlap criterion," *Computer Vision, Graphics, and Image Processing: Graphical Models and Image Processing* 1992;54(5):396-406.

[14] I Kapouleas, A Alavi, W. M. Alves, R. E. Gur and D. W. Weiss, "Registration of three-dimensional MR and PET images of the human brain without markers," *Radiology* 1991;181:731-739.

[15] S. C. Strother , J. R. Anderson, X. L. Xu, J. S. Liow, D. C. Bonar and D. A. Rottenberg, "Quantitative comparisons of image registration techniques based on high-resolution MRI of the brain," *J Comput Assist Tomogr* 1994;18(6):954-962.

[16] A. Venot, J. F. Lebruchec and J. C. Roucayrol, "A new class of similarity measures for robust image registration," *Computer Vision, Graphics, and Image Processing* 1984;28:176-184.

[17] M. Herbin, A. Venot, J. Y. Devaux, E. Walter, J. F. Lebruchec, L. Dubertret and J. C. Roucayrol, "Automated registration of dissimilar images: Application to medical imagery," *Computer Vision, Graphics, and Image Processing* 1989;47:77-88.

[18] C. R. Maurer and J. M. Fitzpatrick, "A review of medical image registration," In: Maciunas RJ, ed. *Interactive Image-Guided Neurosurgery*. Park Ridge, IL: American Association of Neurological Surgeons, 1994;17-44. Neurosurgical Topics.

[19] C. A. Pelizzari, D. N. Levin, G. T. Y. Chen and C. T. Chen, "Image registration based on anatomic surface matching," In: Maciunas RJ, ed. *Interactive Image-Guided Neurosurgery*. Park Ridge, IL: American Association of Neurological Surgeons 1994;47-62. Neurosurgical Topics.

[20] A. C. Evans, T. M. Peters, D. L. Collins, P. Neelin and C. Gabe, "Image registration based on discrete anatomic structures," In: Maciunas RJ, ed. *Interactive Image-Guided Neurosurgery*. Park Ridge, IL: American Association of Neurological Surgeons 1994;63-80. Neurosurgical Topics.

[21] D. A. Weber and M. Ivanovic, "Correlative image registration," *Semin Nucl Med* 1994;24(4):311-323.

[22] B. A. Kall, S. J. Goerss, P. J. Kelly and S. O. Stiving , "Three-dimensional display in the evaluation and performance of neurosurgery without a stereotactic frame: More than a pretty picture? ," *Stereotact Funct Neurosurg* 1994;63:69-75.

[23] J. C. Bezdek, L. O. Hall, L. P. Clarke, "Review of MR image segmentation techniques using pattern recognition," *Med Physics* 1993;20(4):1033-1048.

[24] L. O. Hall, A. M. Bensaid, L. P. Clarke, R. P. Velthuizen, M. L. Silbiger and J. C. Bezdek, "A comparison of neural networks and fuzzy clustering techniques in segmenting magnetic resonance images of the brain," *IEEE Trans on Neural Networks* 1992;2:672-683.

[25] W. H. Press, S. A. Teukolsky, W. T. Vetterling and B. P. Flannery, *Numerical recipes in C. The art of scientific computing.* 2nd ed. New York: Cambridge University Press, 1992.

[26] R. C. Gonzalez and R. E. Woods. *Digital image processing.* Addison-Wesley Publishing Company, 1992.

[27] R. Jain , R. Kasturi and B. G. Schunck. Machine Vision. McGraw-Hill, 1995.

[28] C. A. Davatzikos and J. L. Prince, "An active contour model for mapping the cortex," *IEEE Trans on Medical Imaging* 1995;1:65-80.

[29] F. Maes, A. Collingon, D. Vandermeulen, G. Marchal and P. Suetens, "Multimodality image registration by maximization of mutual information," *IEEE Trans on Med Imag*, Vol 16, No 2 , April 1997.

[30] G. Barequot and M. Shavir , "Partial surface and volume matching in three-dimensions," *IEEE Trans Pat Anal Mach Int*, Vol 19, no 9, September 1997.